Near-surface Qs estimations using multi-channel analysis of surface waves (MASW) and the effect of non-fundamental mode energy on Q-estimation: An example from Yuma Proving Ground, Arizona

Daniel Z. Feigenbaum, Julian Ivanov, Richard D. Miller, Shelby L. Peterie, and Sarah L. C. Morton,*
The University of Kansas and Kansas Geological Survey

Summary

Surface-wave data were collected at the Yuma Proving Ground (YPG) test facility to estimate shear wave velocity using multi-channel analysis of surface waves (MASW). Rayleigh-wave attenuation versus frequency curves were calculated and inverted for shear wave quality factor, Qs. During processing, certain stations created instabilities in the Q-inversion, or produced values that were unrealistic (i.e. minimal or zero attenuation). Therefore, the initial shot gathers were transformed into the FK domain and filtered using higher mode dispersion curves (removing/attenuating the higher-mode energy) to create another set of Qs estimates. The filtered data successfully produced lower Qs estimates without inversion instabilities. The comparison of these results suggest that attenuating higher mode surface wave energy can produce more reliable Qs estimates.

Introduction

Determining the quality (Q) factor of the subsurface was originally proposed by Anderson et al. (1965). The multi-channel analysis of surface waves (MASW) method can be used to determine both (Qs and Qp) shear-wave and compressional-wave quality factor respectively (Ivanov et al., 2014; Xia et al., 2013; Xia et al., 2012). Although the method for Q-estimation was first introduced in the 1960's, the surface-wave energy that is most important for estimating the Q-value was never clarified (e.g. fundamental-mode vs higher-mode energy) (Anderson et al., 1965).

The conventional MASW method can be used to create and invert fundamental mode dispersion curve (phase velocity vs. frequency) images to produce a 2-D shear-wave velocity (Vs) profile. The MASW method was performed on 2-D seismic data collected at the Yuma Proving Ground (YPG) in Arizona. These data were also used to estimate the Quality (Q) values for the near surface (20-30 meters). Q-values are obtained by first evaluating attenuation vs. frequency curves of raw data. Then they are inverted for Q using a-priori Vs, Vp and density information structured in a layered-earth- model (Xia et al., 2012). To date Rayleigh-wave energy has been successfully used to estimate the quality factor in desert (Xia et al., 2002) and glacial conditions (Ivanov et al., 2014). Although, Zhao et al., (2013) was successful in incorporating higher-mode surface waves in the calculation of Q values, we have found that removing the higher-mode energy is beneficial for attenuation curve estimations.

This work utilized a distinctive FK dispersion curve filtering technique (Park et al., 2002) to attenuate higher mode energy and enhance the relative amplitude of the fundamental mode in the seismic data. Our goal was to improve the attenuation-curve estimations sufficiently to achieve more realistic Qs values. Additionally, data were muted in the time domain below the surface waves to remove unwanted noise in the FK domain (Ivanov et al., 2005).

Estimating higher mode energy on the dispersion-curve images, which are used to filter out the higher-mode energy in the FK domain, results in attenuating non-fundamental mode in the space-time domain. Filtered data were then used to generate new attenuation versus frequency curves and obtain different final Q-values. Filtering the data to remove higher mode energy enhanced the Q-value calculations and generates a more realistic result.

Data Acquisition

Multiple 2-D seismic lines were collected at the Yuma Proving Ground in 2009 (Miller et al., 2009a; Miller et al., 2009b). A rubber band assisted weight drop source was used to collect seismic data at 2.4 m shot intervals. The 2-D line was comprised of 4.5 Hz geophones (1.2 m spacing), for a total spread length of 219 m. From this acquisition, a 78 meter rolling spread (Figure 1A) was simulated for Q-estimation.

Methods

The raw shot gathers were muted in time below the surface waves to remove unwanted noise (Ivanov et al., 2005). Dispersion curves were then generated from these muted shot gathers. Dispersion-curve velocities ranged from 70 m/s to 900 m/s, and frequency values of useful signal were observed across a broad frequency range (3 Hz to 90 Hz; Figure 2A). These dispersion curves were used to pick and invert the fundamental-mode surface wave energy (Park et al., 1998; Xia et al., 1999; Miller et al., 1999) to generate a final 2-D velocity depth section (Figure 3A).

The dominate higher-mode energy was identified on the dispersion curves. The frequency-velocity picks were subsequently fed into the dispersion-curve FK filter. The resulting shot gather data possessed greatly enhanced fundamental-mode energy (attenuated higher mode; Figure 1B). Dispersion curves were generated again to allow comparison of how effectively the higher mode was attenuated after the dispersion curve filtering (Figure 2B). The filtered shot gathers were used with the original attenuation curve information to invert for another set of Q-value calculations.

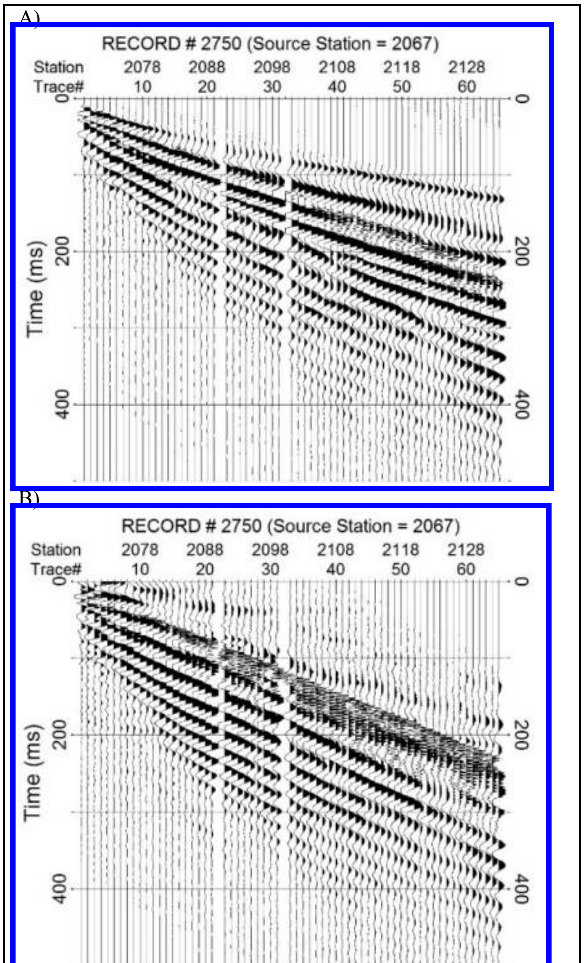

Figure 1: A) Muted shot gather (mute ~400ms to ~800ms) with traces 21 and 31 removed due to receiver noise. B) Shot gather after dispersion-curve FK filter was applied with traces 21 and 31 muted due to receiver noise.

Vp values, were estimated to be ~2.4 times larger than Vs (Xia et al., 2002). Density values (Figure 3B) were derived from the Vp data, using the general form of the density velocity equation (1) (Gardner et al., 1974), where ρ is the density, and Vp is p-wave velocity.

$$\rho = 0.23\,(Vp)^{0.25} \qquad (1)$$

The maximum constraint for the Q-calculations were constrained after multiple attempts to produce a stable solution. It was found that a maximum allowable Qs value of 50 and Qp value of 100 were ideal parameters. Additionally, it has been noted by Xia et al., (2012) that the near surface rarely has Qp values that exceed 100, which is in good agreement with the ideal parameters determined during this study.

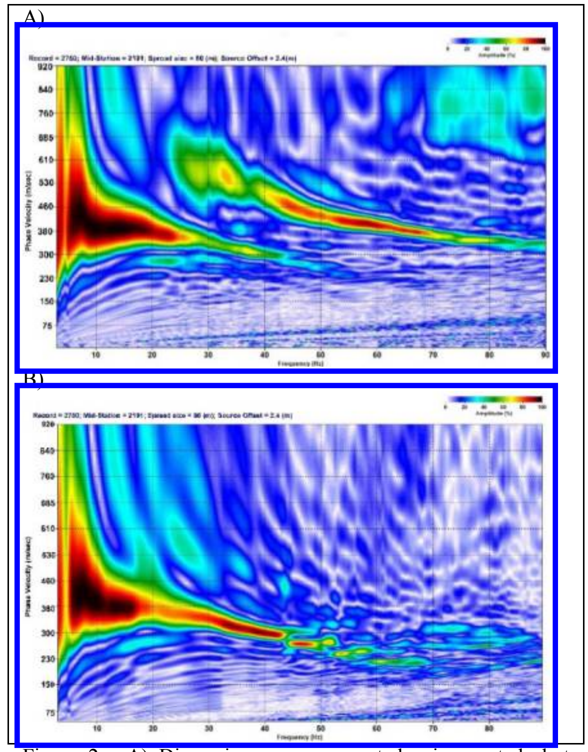

Figure 2: A) Dispersion curve generated using muted shot gathers. Higher mode present masking the fundamental mode energy at frequencies greater than 50-Hz. B) Dispersion curve generated using higher mode dispersion curve filtered data. Higher mode is greatly attenuated, exposing more focused fundamental mode energy as well as energy above 50-Hz.

Results

The inversion results, using the initial attenuation curves, resulted in unrealistically high Qs values (i.e. no attenuation, constant attenuation with depth; Figure 4A). At least one-third of the input attenuation curves generated instabilities during the inversion process. Therefore, they were removed from the final result. The unstable solutions were produced as a result of the Q-inversion calculations diverging or converging (generating a vertical band of zero data and maximum constraint data in the final image respectively).

New attenuation curves were estimated from the filtered seismic data, and different Qs estimates were obtained (Figure 4B). Comparing Figure 4A with 4B, there has been a significant reduction in zones of “no attenuation”. As expected, there appears to be an increase in stability expressed as attenuation varies with depth. Unlike the inversion of attenuation curves generated from unfiltered shot gathers, none of the inversion estimations generated unstable solutions (Figure 4B contains information from every station).

The average reduction in Qs values when comparing Q-estimates generated by the unfiltered versus filtered shot gathers ranged from ~7 to 15. The largest Qs estimate using unfiltered data reached the maximum constraint (50) whereas Q-estimates from the filtered data stabilized at approximately 47.7.

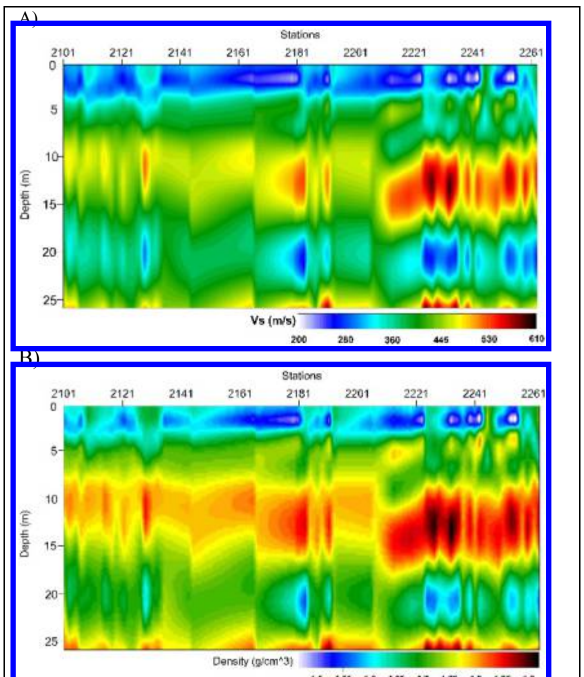

Figure 3: A) 2-D Vs profile estimated from dispersion curve images. B) Density profile calculated from the Vp profile using the density velocity function (1) (Gardner et al., 1974).

Discussion

Station 2101 exhibits an expected attenuation curve (Figure 5A) that experiences a better fit after filtering (Xia et al., 2002; Xia et al., 2012) (i.e. the measured and calculated attenuation curves converge; Figure 5C). Station 2263 displays an irregular attenuation curve (Figure 5B) that also becomes more expected after filtering (Figure 5D) (Ivanov et al., 2014).

Inversions using measured attenuation curves with attenuation increasing with frequency (Xia et al., 2002; Xia et al., 2012) provided a relatively good fit to the calculated curves compared to inversions that use irregular curves (i.e. deviating from the regular trend). Curves that had irregular patterns exhibited a poor fit or no convergence during the inversion process (Ivanov et al., 2014).

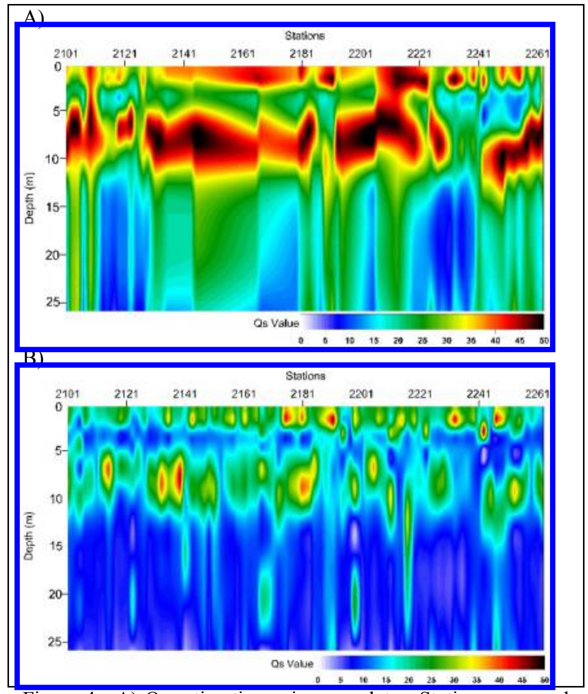

Figure 4: A) Qs estimation using raw data. Stations removed due to estimation “hang” or unrealistic estimation. B) Qs estimation including all stations after higher-mode filtering.

With only unstable solutions higher-mode filtering provides a more stable solution compared to solutions derived from all modes. It is important to note, based on our final test results that there still appear to be instabilities with the Qs calculation as the values do approach the upper limits of acceptable values. However, even as this occurred, the inversion still converged on a solution indicating increased stability.

After the higher-mode energy was filtered out of the muted shot gathers in the FK domain using higher modes, the lateral variability in the final 2-D Qs section is reduced and smoothed. This lateral smoothing indicates stability in the inversion estimations. Lateral instabilities would be observed as high attenuation adjacent to low attenuation zones. Site specific information must be considered to evaluate whether abrupt changes in attenuation is feasible, such as geologic features that would result in such an abnormality. The reduction in these high attenuation zones that neighbor low attenuation zones indicates a trend towards stability. Before the data were filtered, the highest value (50), was reached in the Q-estimation, an indication of an unstable situation. After the data were filtered, the highest value was 47.7. This indicates that the filtered data provided a more stable solution because the Q-inversion converged to a solution before the maximum constraint.

Conclusions

Based on this study, estimating quality (Qs) factor from Rayleigh wave attenuation can be negatively affected by higher mode surface waves. Additionally, these data show how removal of the coherent higher mode surface wave energy was beneficial for not only inversion stability but also in providing more realistic (e.g. lower values) Qs estimates.

More empirical studies of dispersion-curve FK filtering of higher mode surface waves will need to be completed to definitively conclude that dispersion-curve filtering of higher mode energy consistently provides more realistic Qs estimates. Additionally, further work should investigate the effects at other geologic settings. This is important to ensure that the improvement in Qs-estimation is not limited or unique to this field site.

Future work utilizing the high resolution linear radon transform (HRLRT) may prove fruitful in superior delineation of mode energy, as well, which could result in better filtering by dispersion curve in subsequent steps (Luo et al., 2009).

Acknowledgments

The authors of this paper would like to thank the staff and graduate students of the Explorations Services at the Kansas Geological Survey for their contribution. Additionally, we would like to extend our thanks to the field crew who collected the seismic data.

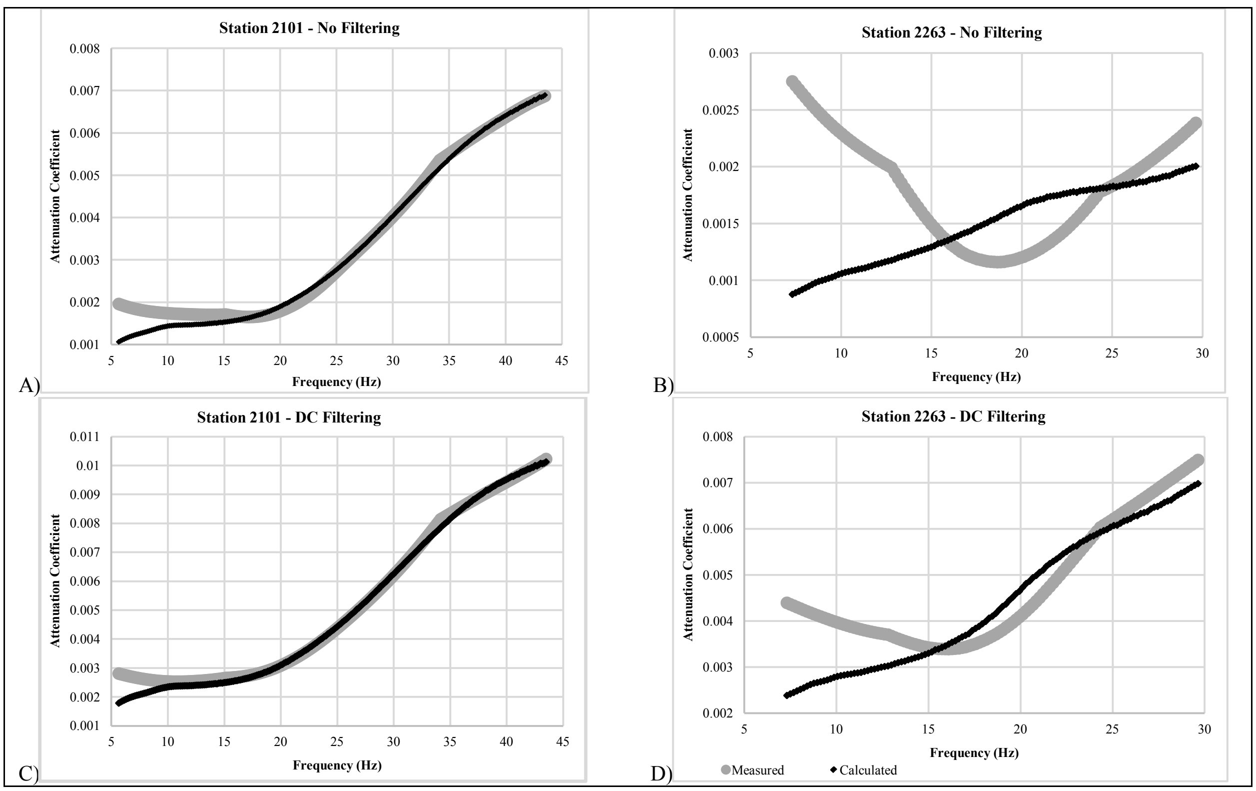

Figure 5: A-D are attenuation curves that were generated from the Q-estimations. These curves show the calculated vs. the observed data. Station 2101 is an example of a “regular” or “expected” attenuation curve. Station 2263 is an example of an “unexpected” or “irregular” attenuation curve. Both attenuation curves improve after dispersion curve filtering. The measured data is displayed in gray circles. The calculated data is displayed smaller/thinner to show the otherwise hidden measured behind.

EDITED REFERENCES

Note: This reference list is a copyedited version of the reference list submitted by the author. Reference lists for the 2016 SEG Technical Program Expanded Abstracts have been copyedited so that references provided with the online metadata for each paper will achieve a high degree of linking to cited sources that appear on the Web.

REFERENCES

Anderson, D. L., Benmenah. A, and, Archambe.Cb, 1965, Attenuation of seismic energy in upper mantle: Journal of Geophysical Research, **70**, 1441–1448, http://dx.doi.org/10.1029/Jz070i006p01441.

Gardner, G. H. F., L. W. Gardner, and A. R. Gregory, 1974, Formation velocity and density — the diagnostic basics for stratigraphic traps: Geophysics, **39**, 770–780, http://dx.doi.org/10.1190/1.1440465.

Ivanov, J., R. D. Miller, S. L. Peterie, and G. Tsoflias, 2014, Near-surface Qs and Qp estimations from Rayleigh waves using multi-channel analysis of surface waves (MASW) at an Arctic ice-sheet site: 84th Annual International Meeting, SEG, Expanded Abstracts, 2006–2012, http://dx.doi.org/10.1190/segam2014-0887.1.

Ivanov, J., C. B. Park, R. D. Miller, and J. Xia, 2005, Analyzing and filtering surface-wave energy by muting shot gathers: Journal of Environmental & Engineering Geophysics, **10**, 307–322, http://dx.doi.org/10.2113/JEEG10.3.307.

Luo, Y. H., J. H. Xia, R. D. Miller, Y. X. Xu, J. P. Liu, and Q. S. Liu, 2009, Rayleigh-wave mode separation by high-resolution linear Radon transform: Geophysical Journal International, **179**, 254–264, http://dx.doi.org/10.1111/j.1365-246X.2009.04277.x.

Miller, R. D., O. M. Metheny, J. M. Anderson, and A. R. Wedel, 2009a, Study of Unconsolidated Sediments at Joint Tunnel Test Range (JTTR) on Yuma Proving Grounds, Arizona: U.S. Geological Survey Open-file Report, **2010-1**, 1–59.

Miller, R. D., S. L. Peterie, B. C. Bennett, B. T. Rickards, J. D. Kearns, O. M. Metheny, A. R. Wedel, B. A. Wedel, and J. M. Anderson, 2009b, Baseline near-surface seismic characterization at the joint tunnel test range (JTTR) on the joint experimentation range complex (JERC) site of the yuma proving grounds, Arizona: U.S. Geological Survey Open-file Report, 2010-2, 1–13.

Miller, R. D., J. Xia, C. B. Park, and J. M. Ivanov, 1999, Multichannel analysis of surface waves to map bedrock: The Leading Edge, **18**, 1392–1396, http://dx.doi.org/10.1190/1.1438226.

Park, C. B., R. D. Miller, and J. Ivanov, 2002, Filtering surface waves: Symposium on the Application of Geophysics to Engineering and Environmental Problems 2002, SEI9-SEI9.

Park, C. B., R. D. Miller, and J. Xia, 1998, Imaging dispersion curves of surface waves on multi-channel record: 68th Annual International Meeting, SEG, Expanded Abstracts, 1, 1377–1380, http://dx.doi.org/10.1190/1.1820161.

Xia, J., C. Shen, and Y. Xu, 2013, Near-surface shear-wave velocities and quality factors derived from high-frequency surface waves: The Leading Edge, **32**, 612–618, http://dx.doi.org/10.1190/tle32060612.1.

Xia, J., Y. Xu, R. D. Miller, and J. Ivanov, 2012, Estimation of near-surface quality factors by constrained inversion of Rayleigh-wave attenuation coefficients: Journal of Applied Geophysics, **82**, 137–144, http://dx.doi.org/10.1016/j.jappgeo.2012.03.003.

Xia, J. H., R. D. Miller, and C. B. Park, 1999, Estimation of near-surface shear-wave velocity by inversion of Rayleigh waves: Geophysics, **64**, 691–700, http://dx.doi.org/10.1190/1.1444578.

Xia, J. H., R. D. Miller, C. B. Park, and G. Tian, 2002, Determining Q of near-surface materials from Rayleigh waves: Journal of Applied Geophysics, **51**, 121–129, http://dx.doi.org/10.1016/S0926-9851(02)00228-8.

Zhao, W., Z. Zhu, Z. Liu, Y. He, and J. Gao, 2013, Estimation of near-surface attenuation using inversion of Rayleigh waves with fundamental and higher modes: 83rd Annual International Meeting, SEG, Expanded Abstracts, 1914–1918, http://dx.doi.org/10.1190/segam2013-0329.1.